(LiOTs), and $[H^+] = 0.10$ mol dm$^{-3}$ as $1.2 \times 10^2$ dm$^3$ mol$^{-1}$ s$^{-1}$. The observed value for $Co(C_2O_4)_3^{3-}$ under the same conditions in the present study is $8.0 \times 10^2$ dm$^3$ mol$^{-1}$ s$^{-1}$, Table I. The enhanced reactivity of $Co(C_2O_4)_3^{3-}$ compared with $Co(NH_3)_5C_2O_4^+$ is probably due to the fact that $Co(C_2O_4)_3^{3-}$ forms a more stable precursor complex than does the positively charged $Co(NH_3)_5(C_2O_4)^+$ complex.

**Acknowledgment.** The authors gratefully acknowledge financial support from the University of Ife Research Committee.

**Registry No.** Ti(III), 22541-75-9; $Co(phen)_3^{3+}$, 18581-79-8; $Co(C_2O_4)_3^{3-}$, 15053-34-6; $Fe(phen)_3^{3+}$, 13479-49-7; $Cl^-$, 16887-00-6; $Br^-$, 24959-67-9.

### References and Notes

(1) J. P. Birk, *Inorg. Chem.*, **14**, 1724 (1975).
(2) A. Adegite and J. F. Ojo, *Inorg. Chem.*, **16**, 477 (1977).
(3) (a) A. H. Martin and E. S. Gould, *Inorg. Chem.*, **14**, 873 (1975); (b) H. J. Price and H. Taube, *ibid.*, **7**, 1 (1968).
(4) G. A. K. Thompson and A. G. Sykes, *Inorg. Chem.*, **15**, 638 (1976).
(5) J. P. Birk and T. P. Logan, *Inorg. Chem.*, **12**, 580, 2464 (1973).
(6) J. D. Ellis and A. G. Sykes, *J. Chem. Soc., Dalton Trans.*, 537, 2553 (1973).
(7) A. Adegite and S. Edeogu, *J. Chem. Soc., Dalton Trans.*, 1203 (1975).
(8) M. Orhanovic and J. E. Earley, *Inorg. Chem.*, **14**, 1478 (1975).
(9) K. L. Scott and A. G. Sykes, *J. Chem. Soc., Dalton Trans.*, 1832 (1972).
(10) A. A. Schilt and R. C. Taylor, *J. Inorg. Nucl. Chem.*, **9**, 211 (1959).
(11) J. C. Bailar, Jr., and E. M. Jones, *Inorg. Synth.*, **1**, 37 (1939).
(12) T. J. Przystas and N. Sutin, *J. Am. Chem. Soc.*, **95**, 5545 (1973).
(13) A. W. Adamson, H. Ogata, J. Grossman, and R. Newbury, *J. Inorg. Nucl. Chem.*, **6**, 319 (1958).
(14) R. K. Wharton, J. F. Ojo, and A. G. Sykes, *J. Chem. Soc., Dalton Trans.*, 1526 (1975).
(15) R. L. Pecsok and A. N. Fletcher, *Inorg. Chem.*, **1**, 155 (1962).
(16) H. Krentzien and F. Brito, *Chem. Abstr.*, **73**, 7865*b* (1970).
(17) A. Adegite, J. F. Iyun, and J. F. Ojo, *J. Chem. Soc., Dalton Trans.*, 115 (1977).
(18) B. Grossman and A. Haim, *J. Am. Chem. Soc.*, **93**, 6490 (1971).
(19) A. Haim and N. Sutin, *J. Am. Chem. Soc.*, **88**, 5343 (1966).
(20) von W. Schneider, *Helv. Chim. Acta*, **46**, 1863 (1963).
(21) E. Bushra and C. H. Johnson, *J. Chem. Soc.*, 1937 (1939).
(22) D. Benson, "Mechanisms of Inorganic Reactions in Solution", McGraw-Hill, New York, N.Y., 1968, p 103.

---

Contribution from the Institut für Anorganische Chemie,
Technische Universität Hannover, D 3000 Hannover, Federal Republic of Germany

# Isomeric Pyrimidinecarboxylic Acids as Electron-Mediating Bridging Ligands in the Inner-Sphere Reduction of Cobalt(III) by Chromium(II)

H. BERTRAM, E. BÖLSING, H. SPIECKER, and K. WIEGHARDT*

*Received July 18, 1977*

The kinetics of the Cr(II) reductions of two binuclear cobalt(III)–ammine complexes containing the isomeric 4- and 5-pyrimidinecarboxylate bridging ligands (I, II) in acidic perchlorate media have been studied. Inner-sphere mechanisms with attack of Cr(II) at a remote ring nitrogen and subsequent electron transfer through the organic ligands are assigned. Since the N-protonated forms of I and II react more rapidly, a radical-ion mechanism is proposed to be operative in both cases, although no direct evidence for the intervention of radical species was obtained. Due to steric hinderance by methyl groups, outer-sphere mechanisms are observed for the Cr(II) and V(II) reductions of the binuclear complex $\mu$-4,6-dimethylpyrimidine-2-carboxylato(*O,O′*)-di-$\mu$-hydroxo-bis[triamminecobalt(III)] and the $\mu$-6-methylpyridine-2-carboxylato(*O,O′*) analogue (complexes III and IV).

## Introduction

In a previous paper, we reported the spectrophotometric detection of a reactive, strongly absorbing intermediate in the reduction of $\mu$-pyrazinecarboxylato(*O,O′*)-di-$\mu$-hydroxo-bis[triamminecobalt(III)] by chromium(II).[1] It was concluded that a coordinated radical is generated during the course of the reduction and that this decays intramolecularly. Due to the intrinsic reducibility of the aromatic, N-heterocyclic ligand, the persistence of the coordinated radical enabled the buildup of detectable concentrations of this species. In the present work we have studied the electron-mediating properties of isomeric pyrimidinecarboxylic acids. The aromatic, heterocyclic acids are easily reduced by chromium(II), probably because of the reduced $\pi$-electron density caused by the presence of two electronegative nitrogen atoms in the ring. It was therefore hoped to find further evidence for the occurrence of the "two-step" reduction mechanism when pyrimidinecarboxylic acids function as electron mediating bridges in the inner-sphere reduction of complexes I–IV by chromium(II).

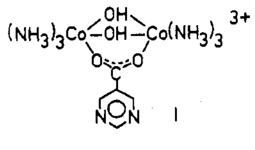

I

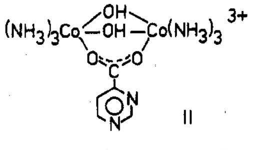

II

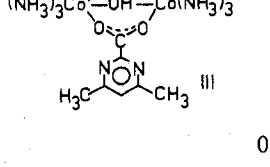

III

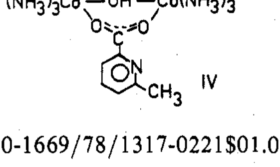

IV

## Experimental Section

**Complexes and Reagents.** The N-heterocyclic ligands were prepared by methods described in the literature: pyrimidine-4-carboxylic acid[2] and pyrimidine-5-carboxylic acid[3] were prepared from the corresponding methylpyrimidines by oxidation with $KMnO_4$ and, likewise, 4,6-dimethylpyrimidine-2-carboxylic acid was prepared from 2-hydroxophenyl-4,6-dimethylpyrimidine[4] and 6-methylpyridine-2-carboxylic acid from lutidine.[5]

The binuclear complexes I–IV were prepared from tri-$\mu$-hydroxo-bis[triamminecobalt(III)] perchlorate in aqueous perchloric acid (0.5 M) following procedures described previously.[6] N-Protonated forms of complexes I–IV were isolated as perchlorate salts. Analytical data are summarized in Table I. The UV–visible spectra of all complexes are very similar ($\lambda_{max}$ 524 nm, $\epsilon$ 110 ± 3 L mol$^{-1}$ cm$^{-1}$). The presence of a symmetrical carboxylate bridge has been confirmed by an x-ray analysis of $\mu$-pyrimidine-5-carboxylato-di-$\mu$-hydroxo-bis[triamminecobalt(III)] perchlorate.[7]

Solutions of $[Cr(H_2O)_6]^{2+}$ and $[V(H_2O)_6]^{2+}$ in perchloric acid were prepared electrolytically as described previously.[1] Lithium perchlorate was obtained from $Li_2CO_3$ and concentrated $HClO_4$ and was recrystallized twice.

**Physical Measurements.** Kinetic runs were followed on a UNICAM SP 1700 spectrophotometer at the first absorption maximum of complexes I, III, and IV ($\lambda_{max}$ 524 nm). Faster runs of the reactions of complexes I and II were followed on a Durrum stopped-flow spectrophotometer. Pseudo-first-order rate constants were obtained from the gradients (×2.303) of plots of log $(A_t - A_\infty)$ vs. time where $A_t$ is the absorbance at time $t$ and $A_\infty$ that after 4–5 half-lives. Such plots were linear to better than 95% completion in all cases.

A protonation constant, $K_1$ (M$^{-1}$), was determined spectrophotometrically ($\lambda$ 285 nm) at 1.0 M ionic strength ($LiClO_4$) for complex I. The value of $K_1 = 13.7 \pm 0.6$ M$^{-1}$ was found to be independent of the temperature (10–41 °C) within experimental error. Complex

0020-1669/78/1317-0221$01.00/0

**Table IV.** Compilation of Kinetic Data of the First Stage of the Cr(II) Reductions and V(II) Reductions of Binuclear Cobalt(III) Complexes Containing an N-Heterocyclic Carboxylic Acid at 25 °C, $\mu = 1.0$ M ($LiClO_4$)

| Complex | $k_a$,[a] $M^{-1}\ s^{-1}$ | $k_b$,[b] $M^{-1}\ s^{-1}$ | $k_{Cr}$,[c] $M^{-1}\ s^{-1}$ | $k_V$,[c] $M^{-1}\ s^{-1}$ | Mechanism[e] | Ref |
|---|---|---|---|---|---|---|
| $\mu$-Pyridine-4-carboxylato[d] | | $0.11 \times 10^3$ | | 0.156 | i.s. | 10 |
| $\mu$-Pyridine-2-carboxylato | | $0.015 \times 10^3$ | | 0.355 | i.s. | 10 |
| $\mu$-Pyrazinecarboxylato | $1.72 \times 10^5$ | $6.6 \times 10^3$ | | | i.s. | 1 |
| I | 3.93[f] | | | 0.198 | i.s. | This work |
| II | $1.74 \times 10^4$ | $2.95 \times 10^3$ | | | i.s. | This work |
| III | | | $9.5 \times 10^{-3}$ | 0.357 | o.s. | This work |
| IV[d] | | | $4.8 \times 10^{-3}$ | 0.221 | o.s. | This work |

[a] The protonated form of complex is the reactive species. [b] The unprotonated form of complex is the reactive species. [c] $[H^+]$-independent path, eq 5. Outer-sphere mechanisms for all V(II) reductions are assigned. [d] Ionic strength 0.5 M ($LiClO_4$). [e] i.s. = inner-sphere and o.s. = outer-sphere mechanism for Cr(II) reductions. [f] Activation parameters: $\Delta H^{\ddagger} = 3.1 \pm 0.1$ kcal mol$^{-1}$; $\Delta S^{\ddagger} = -40.3 \pm 0.4$ cal K$^{-1}$ mol$^{-1}$.

II appears to be a much stronger acid. Therefore, the constant of protonation, $K_{II} = 1.09 \pm 0.2\ M^{-1}$ (25 °C), was determined at an ionic strength of 3.0 M ($LiClO_4$) (λ 290 nm).

Chromium concentrations were determined spectrophotometrically as chromate (λ 372 nm, ε $4.8 \times 10^3$ L mol$^{-1}$ cm$^{-1}$) and solutions of cobalt(II) as $[CoCl_4]^{2-}$ or $[CoCl_3(H_2O)]^-$.

**Determination of Products.** Product analyses of reaction products were carried out by cation-exchange chromatography at 2 °C using the resin Sephadex SP C-25 in the $H^+$ form.

Separation of 1:2 mixtures of I and $[Cr(H_2O)_6]^{2+}$ ($[H^+] = 0.1$ M, $[Cr^{2+}] = 4.05 \times 10^{-3}$ M, $[Co^{III}_2] = 2 \times 10^{-3}$ M, 25 °C) after a reaction time of 90 min yielded four fractions, a–d, which were eluted off the column in that order: (a) a pink band containing only $[Co(H_2O)_6]^{2+}$ (99% of initial cobalt(III)), (b) a blue-gray fraction containing 35% of initial chromium(II) which is believed to be a mixture of $[Cr(H_2O)_6]^{3+}$ and an O-coordinated pyrimidine-5-carboxylatopentaaquochromium(III) species, V, (c) a red band containing 16% of the initial Cr(II) with an elution behavior suggesting an apparent charge of 3+ (The visible spectrum (Table II) is in agreement with a mononuclear N-coordinated pyrimidine-5-carboxylatochromium(III) complex VI.), (d) a blue-green fraction which was eluted off the column with 1.0 M perchloric acid; this contained 49% of initial Cr(II) and has an apparent charge >3+. A binuclear O- and N-coordinated Cr(III) complex with a pyrimidine-5-carboxylato bridging ligand as in VII is consistent with the visible spectrum (Table II).

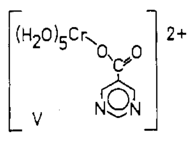

V

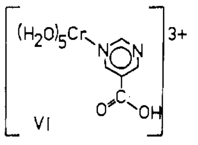

VI

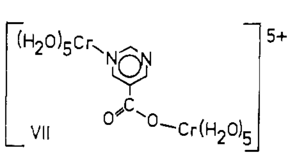

VII

Separation of 1:2 mixtures of complex II and Cr(II) (the same conditions as above were used) after a 2 min reaction time yielded only two fractions: a pink band containing $[Co(H_2O)_6]^{2+}$ (97%) and a blue-gray fraction which could only slowly be eluted off the column with 1.0 M perchloric acid (95% recovery of initial Cr(II)). During elution, the latter species decomposes slowly yielding $[Cr(H_2O)_6]^{3+}$. The visible spectrum of the highly charged species (>3+) (Table II) was obtained by rapid elution using a very short column (1.5 cm) at 2 °C. Identical products were identified from a 1:1 mixture of complex II and Cr(II), except that unreacted binuclear II was eluted off the column after $[Co(H_2O)_6]^{2+}$ (50% of initial cobalt(III)). In this case the reactants were mixed in a stopped-flow apparatus in order to avoid a local excess of Cr(II).

A tentative assignment of structure VIII for the chromium(III)-containing species is based on the similarity of the visible spectrum of complex VII. A binuclear structure in which both Cr(III) ions are coordinated to a nitrogen atom of the pyrimidine ring is not considered to be generated.[8]

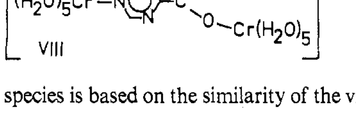

VIII

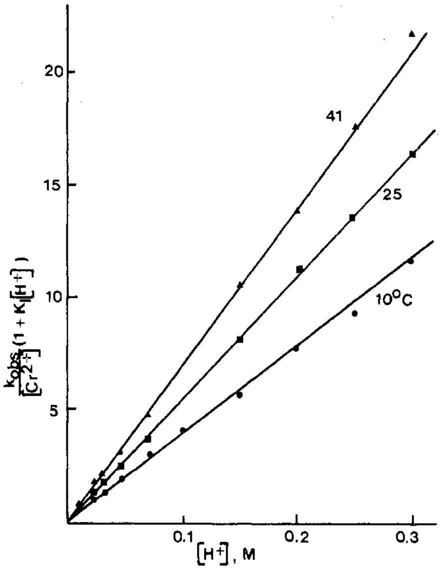

**Figure 1.** Dependence of $(k_{obsd}/[Cr^{2+}])(1 + K_I[H^+])$ on $[H^+]$ for the reduction of $\mu$-pyrimidine-5-carboxylato-di-$\mu$-hydroxo-bis[triamminecobalt(III)] by chromium(II). $K_I$ denotes the spectrophotometrically determined equilibrium constant of protonation of complex I ($13.7 \pm 0.6\ M^{-1}$).

Separation of products of the reduction of complexes III and IV by Cr(II) has not been attempted because of the slowness of the reaction.

**Kinetics of the Reductions of I by Cr(II) and V(II).** From ion-exchange experiments it was shown that the stoichiometry of the reduction of I by Cr(II) is 1:2 (1 mol of complex:1 mol of $[Cr(H_2O)_6]^{2+}$). At 524 nm a single stage of the reaction is observed (decrease of absorbance) during which time both cobalt(III) centers are reduced. Reduction of the first is rate determining. Pseudo-first-order rate constants (excess of Cr(II)), $k_{obsd}$ (s$^{-1}$), are listed in Table III. The reduction of I is first order in $[Cr^{2+}]$ and follows the rate law

$$-d[Co^{III}_2]/dt = k[Cr^{2+}][Co^{III}_2] \tag{1}$$

$$k = \frac{k_a K_I [H^+]}{1 + K_I[H^+]} \tag{2}$$

This is consistent with a mechanism in which the protonated form of I reacts with Cr(II) ($k_a$, $M^{-1}\ s^{-1}$). $K_I$ is the equilibrium constant of protonation. As shown in Figure 1 good linear behavior of $(k_{obsd}/[Cr^{2+}])(1 + K_I[H^+])$ with $[H^+]$ was found at three different temperatures using the spectrophotometrically determined value for $K_I$. The straight lines pass, within experimental error, through the origin indicating that in the $[H^+]$ range employed no significant contribution from the reaction of the unprotonated form with Cr(II) is detected. From the gradients ($k_a K_I$) of the lines, values for $k_a$ were evaluated. Activation parameters were calculated using a nonlinear

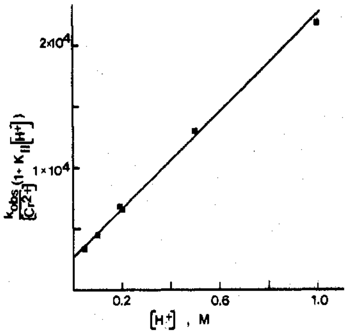

**Figure 2.** Dependence of $(k_{obsd}/[Cr^{2+}])(1 + K_{II}[H^+])$ on $[H^+]$ for the reduction of $\mu$-pyrimidine-4-carboxylato-di-$\mu$-hydroxo-bis[triamminecobalt(III)] by chromium(II). $K_{II}$ is the equilibrium constant of protonation of complex II which was spectrophotometrically determined ($K_{II} = 1.09 \pm 0.08$ $M^{-1}$).

least-squares program. Kinetic data are summarized in Table IV.

The reduction of I by V(II) at 25 °C, $\mu = 1.0$ M ($LiClO_4$), follows the rate law

$$-d[Co^{III}_2]/dt = k_V [Co^{III}_2][V(II)] \tag{3}$$

Reduction of the first Co(III) is again rate determining. The observed second-order rate constant, $k_V = 0.20 \pm 0.01$ $M^{-1}$ $s^{-1}$, is independent of $[H^+]$ (0.03–0.4 M). It is concluded that the reduction of I by V(II) occurs via an outer-sphere mechanism (see Table IV). Using the well-established rate ratio $k_{Cr}/k_V = 0.02$ for outer-sphere reactions of Cr(II) and V(II) with cobalt(III) complexes,[9] it is possible to estimate the second-order rate constant for the outer-sphere reduction of the unprotonated form of I by Cr(II) ($\sim 4 \times 10^{-3}$ $M^{-1}$ $s^{-1}$). This value is small compared with the product $k_a K_I[H^+]$ at the lowest experimental $[H^+]$ concentration used ($\approx 0.54$ $M^{-1}$ $s^{-1}$).

**Reduction of II by Cr(II).** The stoichiometry of the reduction of II by Cr(II) was shown to be 1:2 from ion-exchange experiments. When Cr(II) is in excess a deep green pigment is formed very rapidly. This has been observed previously for the reduction of the analogous $\mu$-pyrazinecarboxylato complex.[1] The reaction is very rapid. Stopped-flow traces of reaction mixtures with the reductant in excess show two distinct stages at λ 524 nm: a rapid increase in absorbance followed by a decrease. The same behavior is observed at 620 nm where the starting complex II does not absorb. In contrast, only a single stage of the reaction is observed at 524 nm, accompanied by a *decrease* in absorbance when II is in excess over reductant. A strictly first-order dependence on $[Cr^{2+}]$ and on $[Co^{III}_2]$ was established for the first stage of the reaction, and a nonlinear dependence on $[H^+]$, irrespective of the actual excess concentration ($[Cr^{2+}]$ or $[Co^{III}_2]$) as in eq 4. This is consistent with the protonated ($k_a$) and unprotonated form ($k_b$) participating in the reduction. $K_{II}$ is the equilibrium constant of protonation. Pseudo-first-order rate constants (excess $Cr^{II}$) are listed in Table III. A plot of $(k_{obsd}/[Cr^{2+}])(1 + K_{II}[H^+])$ vs. $[H^+]$ is linear using the spectrophotometrically determined value for $K_{II}$ (1.09 $M^{-1}$) as is shown in Figure 2. Values for $k_a$ and $k_b$ at 25 °C were determined from the gradient and intercept of the straight line. They are listed in Table IV.

$$\text{rate} = \frac{k_a K_{II}[H^+] + k_b}{1 + K_{II}[H^+]}[Cr^{2+}][Co^{III}_2] \tag{4}$$

The second stage of the reaction (decrease in absorbance at 524 nm) which is observed when Cr(II) is in large excess over the oxidant appears to be independent of $[H^+]$ (0.05–0.5 M) but exhibits a nonlinear dependence on $[Cr^{2+}]$. Since this stage is not involved in the reduction of cobalt(III) centers, a more detailed investigation has not been carried out.

**Reductions of III and IV by Cr(II) and V(II).** Reduction of the first Co(III) center of III and IV is slow and rate determining, irrespective of the reductant (Cr(II) or V(II)). The stoichiometry is 2:1 in all cases (2 mol of reductant and 1 mol of complex) generating $[Co(H_2O)_6]^{2+}$ and Cr(III) or V(III). The kinetics of the reduction of III by V(II) were troubled by the reaction of uncomplexed organic ligand with excess V(II). Therefore, only a limited number of runs were carried out at very low [V(II)].

**Scheme I**

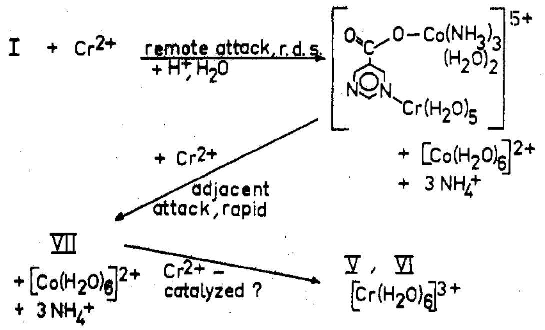

The reductions were found to be independent of hydrogen ion concentration (0.08–0.8 M perchloric acid) and follow the simple second-order rate law

$$-d[Co^{III}_2]/dt = k_{Red}[Co^{III}_2][\text{reductant}] \tag{5}$$

Rate data are compiled in Table IV. From the ratio $k_{Cr}/k_V$ of 0.027 for III and 0.022 for IV it is concluded that the reduction of the first Co(III) of both complexes occurs via outer-sphere mechanisms.

## Discussion

The identification of binuclear Cr(III) complexes, VII and VIII, is regarded as strong evidence that the Cr(II) reductions of both Co(III) ions of I and II occur by an inner-sphere mechanism, respectively. Due to prolonged reaction times of 1:2 mixtures of I and Cr(II) a Cr(II)-catalyzed dissociation of the primary product, VII, may take place generating $[Cr(H_2O)_6]^{3+}$ and the mononuclear fragments V and VI (Scheme I). The very rapid reduction of II prevents a significant contribution from this path (2:1 and 1:1 mixtures). Therefore, no products of dissociation of VIII were detected.

The large increase in absorbance observed at 524 nm in the Cr(II) reduction of II when the reductant is in excess cannot be interpreted in terms of the formation of a Co(III), Cr(III) containing, coordinated radical which would be expected to be formed in a radical-ion mechanism. When the oxidant is in excess, only a single *decrease* in absorbance is observed (a genuine radical–cation intervention should exhibit an increase and a subsequent decrease in absorbance when the radical decays intramolecularly). It is proposed then that the formation of the observed green pigments from VIII with excess Cr(II) is responsible for the increase in absorbance with the rate-determining step being the reduction of the first Co(III) of II. Thus no direct evidence for a two-step mechanism has been obtained for the inner-sphere Cr(II) reductions of I and II.

Interestingly, the protonated forms of I and II react more rapidly (Table IV) with Cr(II) despite an increased positive charge (4+). This behavior has been previously observed for the Cr(II) reduction of the analogous $\mu$-pyrazinecarboxylato complex and could be indicative for a radical-ion mechanism.[1] Note that the ring nitrogens in I are out of conjugation.

Complexes III and IV are reduced by Cr(II) via outer-sphere mechanisms. Because of steric hinderance due to the methyl groups no inner-sphere precursor complex between III or IV and Cr(II) can be formed. The corresponding $\mu$-pyridine-2-carboxylato complex has been shown to react via an inner-sphere mechanism.[10]

**Acknowledgment.** Financial support from the Deutsche Forschungsgemeinschaft and the Fonds der Chemischen Industrie is gratefully acknowledged.

**Registry No.** I, 63985-32-0; II, 64814-03-5; III, 64814-05-7; IV, 64814-07-9; $Cr(H_2O)_6^{2+}$, 20574-26-9; $V(H_2O)_6^{2+}$, 15696-18-1.

**Supplementary Material Available:** Table I showing analytical data of complexes I–IV, Table II showing visible spectra of Cr(III) complexes, and Table III showing kinetic data of Cr(II) reductions of complexes I–IV (5 pages). Ordering information is given on any current masthead page.

## References and Notes

(1) H. Spiecker and K. Wieghardt, *Inorg. Chem.*, **16**, 1290 (1977).
(2) S. Gabriel and J. Colman, *Ber. Dtsch. Chem. Ges.*, **32**, 1536 (1899).
(3) S. Gabriel and J. Colman, *Ber. Dtsch. Chem. Ges.*, **37**, 3649 (1904).
(4) (a) J. Tafel and E. Enoch, *Ber. Dtsch. Chem. Ges.*, **23**, 103 (1890); (b) S. Gabriel and J. Colman, *ibid.*, **32**, 1524 (1899).
(5) A. Ladenburg and K. Scholtze, *Ber. Dtsch. Chem. Ges.*, **33**, 1081 (1900).
(6) K. Wieghardt, *J. Chem. Soc., Dalton Trans.*, 2538 (1973).
(7) G. Maas, *Z. Anorg. Allg. Chem.*, **432**, 203 (1977).
(8) A detailed discussion of this point is given in ref 1.
(9) (a) J. C. Chen and E. S. Gould, *J. Am. Chem. Soc.*, **95**, 5544 (1973); (b) I. Baldea, K. Wieghardt, and A. G. Sykes, *J. Chem. Soc., Dalton Trans.*, 78 (1977).
(10) H. Spiecker and K. Wieghardt, *Inorg. Chem.*, **15**, 909 (1976).

---

Contribution from Physikalisches Institut and Institut für Physikalische Chemie, Universität Erlangen-Nürnberg, D-8520 Erlangen, West Germany, and the School of Chemistry, University of New South Wales, Kensington, New South Wales, Australia 2033

# The High-Spin ($^5T_2$) ⇌ Low-Spin ($^1A_1$) Transition in Solid Bis[2-(2-pyridylamino)-4-(2-pyridyl)thiazole]iron(II) Dinitrate. Its Dependence on Time and on the Previous History of the Specimen

G. RITTER,[1a] E. KÖNIG,*[1b] W. IRLER,[1a] and H. A. GOODWIN[2]

*Received April 6, 1977*

The continuous high-spin ($^5T_2$) ⇌ low-spin ($^1A_1$) transition in $^{57}$Fe-enriched (>90%) solid $[Fe(paptH)_2](NO_3)_2$ (paptH = 2-(2-pyridylamino)-4-(2-pyridyl)thiazole) has been studied in detail by Mössbauer spectroscopy. When the sample is cooled slowly, the transition is almost complete, the $^5T_2$ fraction at 290 and 105 K being >0.95 and 0.067, respectively. A pronounced hysteresis of $\Delta T_c = 34$ K has been observed, the transition being centered at $T_c^{>} = 263$ K for increasing temperature and at $T_c^{<} = 229$ K for decreasing temperature. When the sample is cooled rapidly, a considerable fraction (~0.40) of the $^5T_2$ state molecules is metastable at 105 K. Subsequent heating causes a high-spin ($^5T_2$) → low-spin ($^1A_1$) transformation to the "equilibrium" composition. The kinetics of this transformation were studied at 160, 170, and 180 K. The resulting mean lifetimes for the $^5T_2$ state are, serially, $\tau$ = 14 460, 5590, and 1160 s. The activation energy for the process is $\Delta E$ = 7.5 kcal mol$^{-1}$. Various other high-spin ($^5T_2$) ⇌ low-spin ($^1A_1$) systems have been studied for similar nonequilibrium behavior with negative results.

## Introduction

It has been suggested previously[3] that, on the basis of magnetic susceptibilities between about 80 and 380 K and visual color changes, several iron(II) complexes of the tridentate ligand 2-(2-pyridylamino)-4-(2-pyridyl)thiazole (abbreviated paptH) exhibit high-spin ($^5T_2$) ⇌ low-spin ($^1A_1$) transitions as solids. This inference has recently been confirmed[4] by $^{57}$Fe Mössbauer-effect studies on absorbers enriched to >90% $^{57}$Fe of $[Fe(paptH)_2]X_2{\cdot}H_2O$, where X = $NO_3$ and $ClO_4$. As in several other $[Fe^{II}{-}N_6]$ systems studied previously,[5-8] the high-spin ($^5T_2$) ⇌ low-spin ($^1A_1$) transition in these complexes extends over a considerable range of temperature and is incomplete at cryogenic temperatures.

In the course of the initial studies,[3] a marked time dependence of the magnetism of $[Fe(paptH)_2](NO_3)_2$ was noted, the origin of which having been attributed to a slow phase change accompanying the change from high-spin ($^5T_2$) to low-spin ($^1A_1$) ground state. If confirmed, this observation might prove to be of importance with respect to the mechanism of high-spin ($^5T_2$) ⇌ low-spin ($^1A_1$) transitions in solid iron(II) complexes. Therefore, in the present study, we report the results of a detailed investigation, by the $^{57}$Fe Mössbauer effect, of the dependence of the high-spin ($^5T_2$) ⇌ low-spin ($^1A_1$) transition in enriched absorbers of $[Fe(paptH)_2](NO_3)_2$ on both time and the previous history of the specimen.

## Experimental Section

The sample of $[Fe(paptH)_2](NO_3)_2$ was prepared as described elsewhere,[3] employing iron metal enriched to >90% in $^{57}$Fe as the starting material. The homogeneity and purity of the product were verified by chemical analyses, magnetism, and the Mössbauer spectra reported below.

Mössbauer spectra were measured with a spectrometer of the constant-acceleration type (Frieseke und Hoepfner FHT 800A), operating in the multiscaler mode. The absorber was of polycrystalline form and contained 0.63 mg/cm$^2$ of $^{57}$Fe. A 50 mCi source of $^{57}$Co in rhodium was used, the calibration being effected with a metallic-iron absorber. All velocity scales and isomer shifts are referred to the iron standard at 298 K. To convert to the sodium nitroprusside scale add +0.257 mm s$^{-1}$. Movement of the source toward the absorber corresponds to positive velocities. Variable-temperature measurements between 105 and 290 K were obtained by the use of a small heating coil with the sample placed in a superinsulated cryostat. The temperatures were carefully monitored by means of a calibrated copper/constantan thermocouple, a cryogenic temperature controller (Artronix Model 5301-E), and liquid nitrogen as coolant. In order to determine reliable values for the effective thickness, all measurements were performed with the identical geometrical arrangement for source, absorber, and detector. The resulting data were carefully corrected for nonresonant background of the $\gamma$ rays and computer-fitted to Lorentzian line shapes. The utilization of a sample enriched in $^{57}$Fe allowed the relatively rapid accumulation of spectra, and hence measurement of the time dependence of the spectral characteristics became feasible. The quality of the measurements is demonstrated in Figure 1, in which the diagram on the left (a) shows a spectrum accumulated within 15 min, whereas the diagram on the right (b) shows data collected over a period of 60 min. Here the vertical bars indicate the magnitude of the statistical error. Evidently, the spectrum displayed on the left (a) is sufficiently accurate for the present purposes.

To obtain values of the effective thickness $t_{^5T_2}$ and $t_{^1A_1}$, the well-known area method[9,10] has been used. In the Mössbauer spectrum of an absorber of finite thickness, the normalized area[10] for the $i$th line is determined by eq 1, provided the lines are well resolved. Here

$$A_i = {}^1/_2\pi f_S \Gamma_i L(t_i) \qquad (1)$$

$\Gamma_i$ is the line width of the $i$th absorber line and $f_S$ is the Debye–Waller factor of the source. Also, $A_i$ is independent of the line shape of the source. For a Lorentzian line shape of the absorber line, the saturation function $L(t_i)$ assumes the form[9]

$$L(t_i) = t_i e^{-t_i/2}\,[I_0(t_i/2) + I_1(t_i/2)] \qquad (2)$$

where $I_\gamma$ are the Bessel functions with an imaginary argument.

In order to determine, from the quantity $A_i$, the effective thickness $t_i$, the inverse function $t_i(L)$ is required. This function is given in numerical form by eq 3.[11] For $0 \le t_i \le 8$, the accuracy of eq 3 is

$$t_i(L) = 3.2250L - 8.2620 + (8.9679L^2 - 36.8464L + 68.2803)^{1/2} \qquad (3)$$

0020-1669/78/1317-0224$01.00/0